Finite element computation of woven ply laminated composite structures up to rupture

Cyril Bordreuil, Christian Hochard

Finite Element Computation of Woven Ply Laminated Composite Structures up to Rupture

CYRIL BORDREUIL and CHRISTIAN HOCHARD
Laboratoire de Mécanique et d'Acoustique, 31, Chemin Joseph Aiguier, 13402 Marseille Cedex 20, France. e-mail: cyril_bordreuil@yahoo.fr, hochard@unimeca.univ-mrs.fr

Abstract. For unidirectional ply laminates, the great diversity of the damage mechanisms and their patterns of evolution make it extremely difficult to estimate the strength margins. In the case of *woven* ply laminates, the number of damage mechanisms is fairly small (no transverse rupture occurs and the material has a greater resistance to delamination) and the behaviour of the material is fairly simple to model up to rupture. In this study, a numerical model for woven ply laminated composite structures up to rupture is developed. The implementation is performed in a Euler Backward scheme and the consistent tangent stiffness matrix is calculated. Comparison with some experiments on structures are made and the model predicts these experiments well.

Key words: woven composite, finite element, rupture, damage.

1. Introduction

When unidirectional (UD) ply laminates are subjected to severe loading up to rupture, many mechanisms responsible for the damage and rupture occur on different scales: matrix micro-cracking, fibre/matrix debonding, transverse rupture, fibre rupture, delamination, rupture of the plies and the laminate [1]. The great diversity of the damage mechanisms and their patterns of evolution make it extremely difficult to estimate the strength margins.

In the case of *woven* ply laminates, the number of damage mechanisms is fairly small (no transverse rupture occurs and the material has a greater resistance to delamination) and the behaviour of the material is fairly simple to model up to rupture [2]. A finite element calculation in terms of plane stresses which includes the plastic elastic damage behaviour of the woven ply laminates makes it possible to describe the rupture of a structure. A prototype code was carried out on the Matlab software and a comparison with an experimental test on perforated plate made it possible to validate this assumption [3].

The behaviour of this material is strongly non-linear (damage, anelastic strain, rupture) and the prototype software constructed on Matlab is not adapted to use in engineering and design department for structure optimization. The purpose of this paper is to integrate the behaviour in high-efficiency numerical tools in order to

optimize structure components. Optimization needs low time computation in order to search for an effective solution.

The numerical implementation of combined damage and elastic-plastic behaviour is not a simple task. Some algorithms coupling damage and plasticity are present in plane stress models [4] and [5], in implicit schemes. Here, the implementation of an elastic plastic damage model with some orthotropic characteristics is developed.

The behaviour of the woven ply is then implemented in the commercial software Abaqus via a user subroutine `umat`. The two important points in the computation are the local algorithm and the consistent tangent matrix [6]. Again, comparisons are made between the results of experimental tests and those of finite element simulations involving a plate with a hole subjected to tensile tests.

To save time, the local algorithm is linearized, and a consistent tangent operator is implemented.

2. Woven Ply Laminates

Woven ply laminates have weaker mechanical characteristics and are more expensive than UD ply laminates. However, they are used in industry, for example, to make helicopter blade skins because they are not subjected to transverse rupture. In addition, these materials are more resistant to delamination. The number of damage mechanisms liable to occur is thus reduced and the behaviour of the material is easier to model up to rupture. A finite element calculation in terms of the plane stresses, which includes the plastic elastic damage behaviour of the woven ply material, can be used to describe the rupture of a structure of this kind. In general, the rupture of a ply leads to the rupture of the laminate in the case of woven plies. The structure of the woven ply is shown in Figure 1.

The structure of the material is periodic. The macroscopic model sees the material as a continuum.

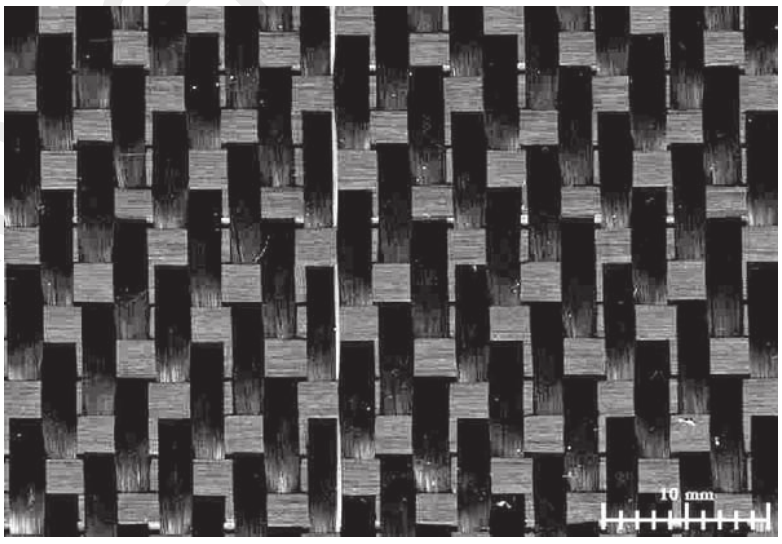

Figure 1. Structure of the woven ply, satin 4.

The behaviour of materials of this type and the modelling procedure used were previously described in [2]. Here, the main points of the model are recalled. The material was reinforced with a carbon fabric of the four-harness satin type with balanced warp and fill yarns. In the fibre directions, the woven ply showed a brittle linear elastic behaviour when subjected to tension (see Figure 2). The damage occurring in these directions did not affect the behaviour of the ply under traction loading. However, traction applied to the warp direction generated micro cracks in the matrix within both the fill and warp yarns. When shear loading was applied from a tensile test on a $[45]_8$ laminate, a decrease in the shear modulus as well as anelastic strains were observed (see Figure 2). The decrease in the modulus was due to the ply shear stress, which generated some fibre/matrix decohesion and matrix micro-cracks within the warp and fill yarns. These micro-cracks, which are mainly located at the fibre/matrix interfaces, are assumed to run parallel to the fill and warp directions. The anelastic strains and the loading-unloading hysteresis observed (Figure 2) were mainly due to the slipping/friction processes occurring between the fibres and matrix as the result of the damage.

We adapted the meso scale model developed for UD plies described in [7] to woven ply laminates. This model was designed for dealing with woven plies with balanced or non-balanced warp and fill yarns. The damage kinematics adopted were based on the following three internal damage variables (d_1, d_2, d_{12}) with the brittle fracture of fibres in the warp and fill directions and the decreasing stiffness under shear loading, respectively. The gradual development of the damage d_{12} depends on the shear load as well as the traction load, which generates micro-cracks.

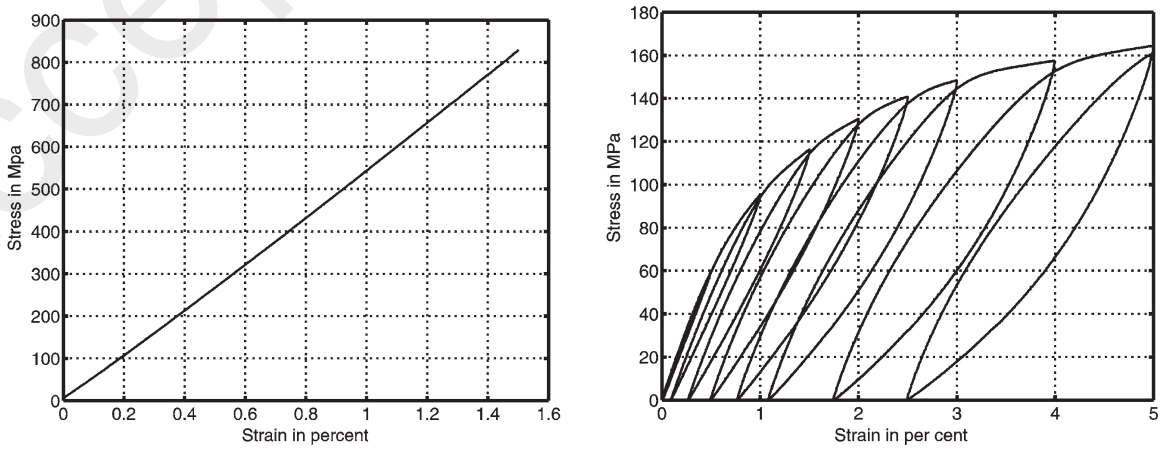

(a) (b)

Figure 2. Tensile test performed in the fibre (a) and shear direction (b).

Under the assumption of plane stresses and small perturbations, we can write the strain energy of the woven ply in the form of Equation (1),

$$E_D = \frac{1}{2}\left[\frac{\langle\sigma_1\rangle_+^2}{E_1^0(1-d_1)} + \frac{\langle\sigma_1\rangle_-^2}{E_1^0} - 2\frac{\nu_{12}}{E_1^0}\sigma_1\sigma_2 + \right. \\ \left. + \frac{\langle\sigma_2\rangle_+^2}{E_2^0(1-d_2)} + \frac{\langle\sigma_2\rangle_-^2}{E_2^0} + \frac{\sigma_{12}^2}{G_0^{12}(1-d_{12})}\right], \tag{1}$$

where $\langle.\rangle_+$ is positive and $\langle.\rangle_-$ is negative. The tension and compression energy are split in order to describe the unilateral features due to the opening and closing of the micro-defects. From this potential, thermodynamic forces associated with the tension and shear internal variables d_i ($i = 1$ and 2) and d_{12} are defined:

$$Y_{d_i} = \frac{\partial E_D}{\partial d_i} = \frac{\langle\sigma_i\rangle_+^2}{2E_i^0(1-d_i)}, \tag{2}$$

$$Y_{d_{12}} = \frac{\partial E_D}{\partial d_{12}} = \frac{\sigma_{12}^2}{2G_{12}^0(1-d_{12})}. \tag{3}$$

The development of the internal variables depends on these thermodynamic forces and more precisely on their maximum values during the history of the loading.

In traction, the development of d_1 and d_2 is severe in order to represent the brittle behaviours according to the warp and the fill directions. To take into account the traction/shear coupling during the development of d_{12}, we define the equivalent thermodynamic force and the maximum value of this force during the history of the loading:

$$Y = \alpha_1 Y_{d_1} + \alpha_2 Y_{d_2} + Y_{d_{12}}, \tag{4}$$

where α_1 and α_2 are the tension/shear coupling constants. It should be noted that this equivalent force which governs the development of the progressive damage variable d_{12} does not depend on the compression stresses in the warp and fill directions. As for the unidirectional plies, a linear law with respect to the square root of Y is chosen to describe the damage variable development:

$$d_{12} = \frac{\sqrt{Y} - \sqrt{Y_0}}{\sqrt{Y_c} - \sqrt{Y_0}}, \tag{5}$$

$$d_i = 0 \quad \text{if } Y_{d_i} < Y_{if} \quad \text{else } d_i = 1, \tag{6}$$

where the constant parameters Y_0 and Y_c correspond to the threshold and the critical value of the development of d_{12} which varies from 0 to 1. Y_{1f} and Y_{2f} are the parameters which define the ultimate forces in the warp and fill directions.

After loading on a laminate $[45]_8$ (Figure 2), anelastic strains are observed. These strains can be linked to the slipping/friction phenomena between the fibres and matrix as a consequence of the damage. Because of the warp and fill fibre

directions, which prevent traction anelastic strains, only the shear anelastic strains are significant. We described these strains by a plastic hardening model. The coupling between the damage and plasticity is taken into account by using the effective stress and strain, which are defined as:

$$\tilde{\sigma}_{12}\dot{\tilde{\varepsilon}}^{p}_{12} = \sigma_{12}\dot{\varepsilon}^{p}_{12}, \tag{7}$$

$$\tilde{\sigma}_{12} = \frac{\sigma_{12}}{1 - d_{12}}, \tag{8}$$

$$\dot{\tilde{\varepsilon}}^{p}_{12} = \dot{\varepsilon}^{p}_{12}(1 - d_{12}). \tag{9}$$

It is assumed that the stresses σ_1 and σ_2 do not influence the elastic field defined by:

$$f(\tilde{\sigma}_{12}, p) = |\tilde{\sigma}_{12}| - R(p) + R_0, \tag{10}$$

where R_0 represents the initial threshold for the anelastic strain and $R(p)$ is the hardening function of the accumulated anelastic strain p chosen such as:

$$R(p) = Kp^{\gamma}, \tag{11}$$

where K is the power law coefficient and γ is the power law exponent. Here p is defined by:

$$\dot{p} = (1 - d_{12})|\dot{\gamma}_{12}|. \tag{12}$$

The loading-unloading hysteresis, which is mainly due to the slipping/friction phenomena between the fibres and matrix, is not modelled.

3. A Previous Study

A previous work studied the possibility of using such a model to predict the behaviour of a structure up to rupture [3]. It was tested on a woven ply laminated plate $[+45, -45]_s$ with a hole.

To evaluate the prediction of the model more precisely, local measures were performed with the help of strain gauges. The strain gauges are located as shown in Figure 3.

In Figure 4, the experimental results was shown that the level of strength resistance was well predicted by the simulation. This prototype code was implemented in Matlab to show the feasibility of the coding.

In this study, an efficient numerical model is developped and implemented in Abaqus software.

4. Numerical Implementation

The numerical implementation is developed here. In the case of an implicit resolution of the virtual work principle, the two main points are (i) the computation of

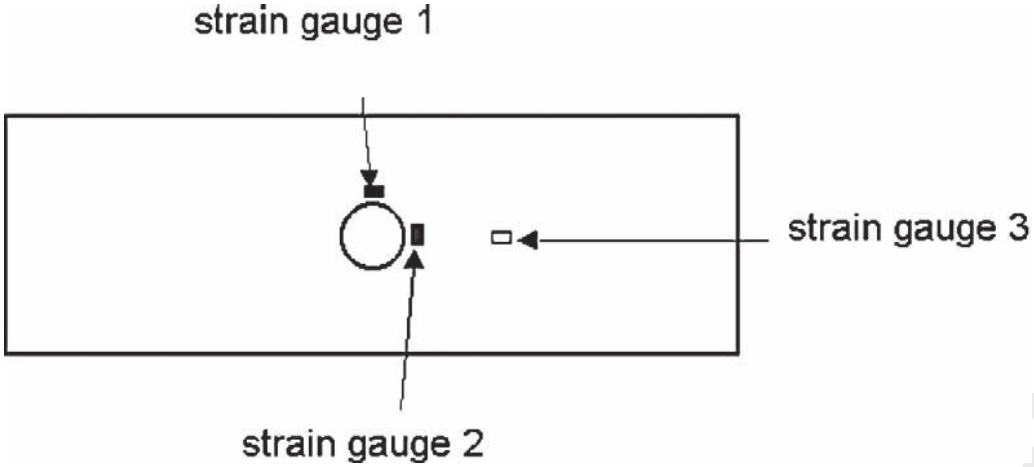

Figure 3. Location of strain gauge measurements.

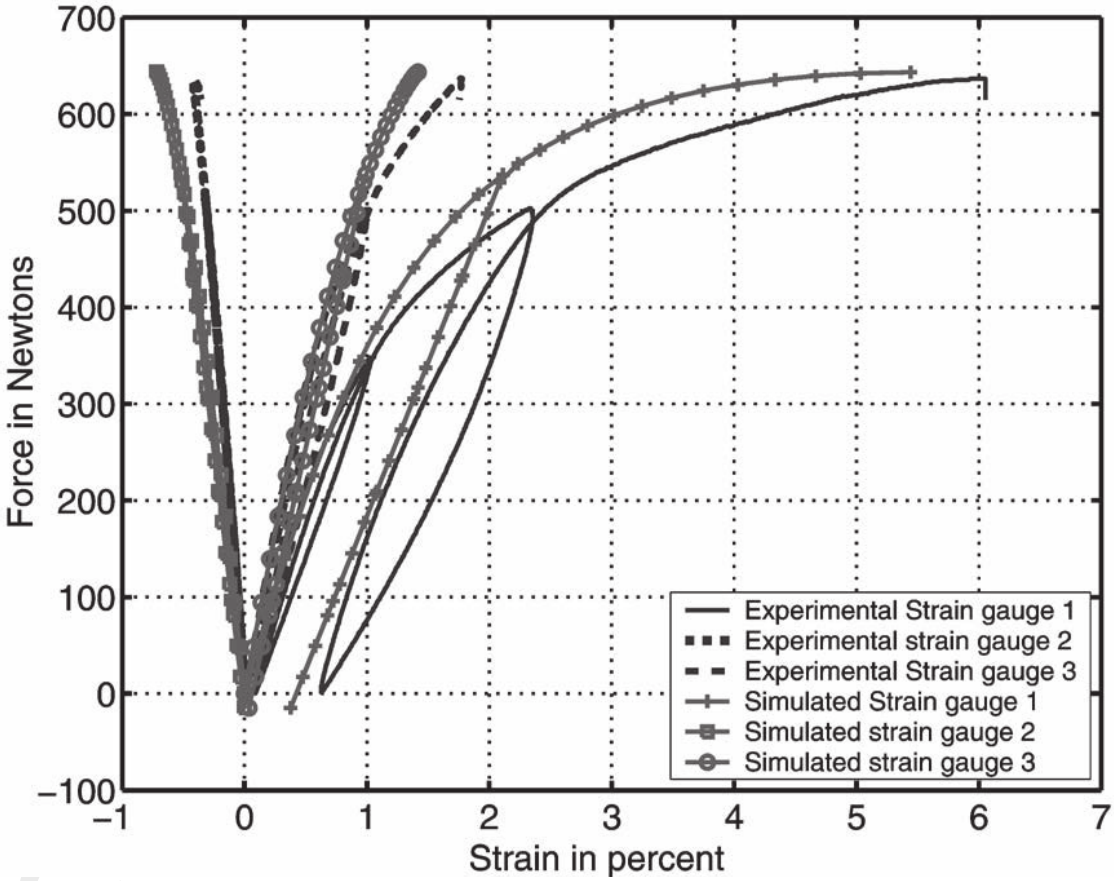

Figure 4. Comparison of measurements and simulation for $[+45, -45]_s$ laminate.

the stresses in the local algorithm and (ii) the computation of the consistent tangent operator in order to maintain the second order rate of convergence.

The model introduced different non-linearities which were induced by the damage and anelastic strain. The fact that woven plies can not support anelastic strains in the direction of the fibres simplifies the algorithm.

In the first section, the previous woven plies model is described in an incremental framework for the local algorithm. Following this, the way to obtain the consistent matrix is then deduced.

Table I. The unknown state dependent variables.

Unknown variables
$\sigma_{n+1}, d_{12_{n+1}}, p_{n+1}$

4.1. INCREMENTAL MODEL

The notations are such that $_{n+1}$ represents the values of the variables at the end of the time step. The upper-script ^{e} is for elastic strain and ^{p} is plastic (or anelastic) strain.

The incremental model is developed in a Euler Backward scheme. The Euler Backward is chosen for its high stability. The unknown variables of the model are listed in Table I.

All these variables need to be updated for a time step. Variables d_i are not treated because the material does not damage in the direction of the fibre until brittle fracture occurs, although a criterion is developped for the rupture in the direction of the fibre.

The stresses are ordered in the Voigt notation ($\varepsilon_1 = \varepsilon_{11}, \varepsilon_2 = \varepsilon_{22}, \gamma_{12} = 2\varepsilon_{12}$). In the direction of the fibre the stresses are given by:

$$\sigma_i = c_{ij}\varepsilon_i \quad \text{for } i = 1, 2. \tag{13}$$

In this study, non-linear elasticity in compression due to micro buckling or alignment of the fibre is not taken into account. The shear stresses are determined with the help of the elastic relationship:

$$\sigma_{12_{n+1}} = G^0_{12}(1 - d_{12_{n+1}})\gamma^{e}_{12_{n+1}}. \tag{14}$$

The different elastic strains are obtained by:

$$\varepsilon^{e}_{1_{n+1}} = \varepsilon^{e}_{1_n} + \Delta\varepsilon_1, \tag{15}$$
$$\varepsilon^{e}_{2_{n+1}} = \varepsilon^{e}_{2_n} + \Delta\varepsilon_2, \tag{16}$$
$$\gamma^{e}_{12_{n+1}} = \gamma^{e}_{12_n} + \Delta\gamma^{e}_{12}. \tag{17}$$

The two main strains are obtained by the summation of total incremental strains as long as no damage or no anelastic strain are possible until rupture. The elastic shear strain is obtained by computing the difference of the total strain and the plastic strain:

$$\Delta\gamma^{e}_{12} = \Delta\gamma_{12} - \Delta\gamma^{p}_{12}. \tag{18}$$

The main features in computing stresses are the values of the damage at the end of the increment and of the incremental plastic strain. Damage is given by the equation:

$$d_{12_{n+1}} = \frac{\sqrt{Y_{n+1}} - \sqrt{Y_0}}{\sqrt{Y_c} - \sqrt{Y_0}}, \tag{19}$$

where

$$Y_{n+1} = \sup\left(\frac{G_{12}^0}{2}(\gamma_{12_{n+1}}^e)^2 + \alpha_1 Y_{d_1} + \alpha_2 Y_{d_2}, Y_n\right). \tag{20}$$

If the first term is greater than Y_n, then damage will evolve.

If this set of equations is expressed in a displacement based problem, the solution is function of incremental strains. When plasticity is involved, the shear strain increment is then decomposed as in Equation (18) and the only unknown variable is $\Delta\gamma_{12}^p$. When plasticity occurs, the overall set of equations must be linearised with respect to the unknown variable (more details of the linearisation can be found in Appendix).

The first search is to establish whether or not plasticity occurs due to a predictor step at fixed internal variables (d_{12_n}, p_n). If plasticity occurs the equation has to be solved for the unknown variable $\Delta\gamma_{12}^p$ and a Newton method developed. The stress state has to be on the yield surface at the end of the time step determined by:

$$f_{n+1} = |\tilde{\sigma}_{12_{n+1}}| - R_0 - K p_{n+1}^{\gamma}, \tag{21}$$

where the equivalent plastic strain is computed by

$$\Delta p = (1 - d_{12_{n+\beta}})|\Delta\gamma_{12}^p|, \tag{22}$$

where the value of the damage variable is calculated as

$$d_{12_{n+\beta}} = (1-\beta)d_{12_n} + \beta d_{12_{n+1}}. \tag{23}$$

To find the unknown variable, Equation (21) is linearised so that

$$\partial f = J_{dp}(\partial\tilde{\sigma}_{12_{n+1}}) - K\gamma p_{n+1}^{\gamma-1}\partial p, \tag{24}$$

where J_{dp} is an indicator of the sign of the effective stress ($J_{dp} = 1$ if $\tilde{\sigma}_{12} > 0$, $J_{dp} = -1$ otherwise) and where the variation of effective stress (Equation (8)) is expressed as:

$$\partial\tilde{\sigma}_{12_{n+1}} = G_{12}^0\partial(\gamma_{12_n}^e + \Delta\gamma_{12}^e). \tag{25}$$

The elastic strain variation is expressed with relation to the plastic incremental strain

$$\partial\gamma_{n+1}^e = \partial\Delta\gamma^e = -\partial\Delta\gamma^p \tag{26}$$

for a total fixed incremental strain. The damage variation gives:

$$\partial d = \frac{1}{2}\frac{1}{\sqrt{Y}(\sqrt{Y_c} - \sqrt{Y_0})}\partial Y_{d_{12}} \tag{27}$$

as long as total strains are fixed ($\partial Y_{d_1} = \partial Y_{d_2} = 0$ in the local algorithm), when damage evolves. If no evolution of damage occurs then:

$$\partial d = 0. \tag{28}$$

With the definition of $\sqrt{Y}$ expressed by the elastic shear strain, we write:

$$\partial Y_{d12} = G^0_{12}\gamma^{\mathrm{e}}_{12_{n+1}}\partial\gamma^{\mathrm{e}}_{12_{n+1}}. \tag{29}$$

To finish the linearisation, the equivalent plastic strain has to be linearised:

$$\partial p = J_{\mathrm{ep}}\partial\gamma^{\mathrm{p}}_{12}(1 - d_{12_{n+\beta}}) - |\Delta\gamma^{\mathrm{p}}_{12}|\partial d_{12_{n+\beta}} \tag{30}$$

where J_{ep} is an indicator of the sign of $\Delta\gamma^{\mathrm{p}}_{12}$ and with

$$\partial d_{12_{n+\beta}} = \beta\partial d_{12_{n+1}} J_{\mathrm{d}} \tag{31}$$

where J_{d} is an indicator of damage. If damage evolves then $J_{\mathrm{d}} = 1$ otherwise $J_{\mathrm{d}} = 0$. The function to be solved is such that:

$$\frac{\partial f}{\partial\gamma^{\mathrm{p}}} = -J_{\mathrm{dp}}G^0_{12} - K\gamma p^{\gamma-1}\Bigg(J_{\mathrm{ep}}(1 - d_{12_{n+\beta}}) + \\ + |\Delta\varepsilon^{\mathrm{p}}_{12}|\frac{\beta}{2}J_{\mathrm{d}}\frac{G^0_{12}\gamma^{\mathrm{e}}_{12_{n+1}}}{\sqrt{Y_{n+1}}(\sqrt{Y_c} - \sqrt{Y_0})}\Bigg). \tag{32}$$

The correction is found by:

$$c^{\mathrm{p}} = -f/(\partial f/\partial\gamma^{\mathrm{p}}). \tag{33}$$

The scheme is iterated until the solution is found: $f_{n+1} = 0$. The scheme is summarised in Table II.

4.2. RUPTURE CRITERION

Two types of rupture are observed with the developed model. The first one is due to the progressive loss of rigidity of the material in the shear direction. The second one is due to brittle rupture in the direction of the fibres. From the point of view of implementation, the first one does not need any criteria but the second one has to be expressed in terms of rupture criteria. At this point, a criterion in a maximum conjugate damage variable is chosen and, because no damage is involved before rupture, it is equivalent to a stress criterion.

Table II. Local algorithm.

1.	Elastic predictor $\sigma^{\mathrm{el}} = \sigma_n + \mathbf{C} : \Delta\varepsilon$.
2.	Test the rupture criterion in the direction of the fibre. If criterion overlapps: New time step = .5× old time step and go to 6.
3.	$test = f(\sigma^{\mathrm{el}}, p_n, d_{12_n})$.
4.	Check if plasticity occurs: $test > tolor$ then (a) compute $\frac{\partial f}{\partial \varepsilon^{\mathrm{p}}}$, (b) calculate c_p, (c) update internal variables p_{n+1} and d_{n+1}, (d) update stress: $\sigma_{n+1} = \sigma_n + \mathbf{C} : (\Delta\varepsilon - \Delta\varepsilon^{\mathrm{p}})$, (e) calculate $test = f_{n+1}$ and go to 4.
5.	Update internal variables.
6.	Compute consistent tangent matrix.
7.	End of the computation.

From the point of view of the Euler Backward, the time step has to be recomputed each time the criterion is overlapped:

$$Y_{d_i} > Y_{i_{\mathrm{f}}}. \tag{34}$$

As long as the stresses shut down to zero when rupture (brittle fracture) is encountered the calculus is stopped due to loss of convergence of the iterative scheme. In this model, it is assumed that when one ply reaches the critical stress then the whole laminate is ruptured.

It is important to note that the overall behaviour that of brittle fracture plus shear damage is embedded in the model.

4.3. CONSISTENT TANGENT

Simo and Taylor [6] have shown that to keep good computational efficiency, namely good rate of convergence with the principle of virtual work, the incremental consistent matrix must be computed: $\frac{\partial \Delta\sigma}{\partial \Delta\varepsilon}$. In most cases (anisotropic behavior, large number of internal variables, ...), this computation is not an easy task. In our specific case, the difficulties arise from the thermodynamic conjugate force of the damage Y_{d_i}. For the sake of simplicity, the computation of the consistent matrix is calculated in the case of an elastic damage behaviour and then it is applied to our plasticity model.

4.3.1. *Elastic Damage Behaviour*

The first part of the consistent tangent is obtained for the main strains and stresses. From Equation (13), the component of the tangent matrix is obtained by:

$$\left(\frac{\partial \sigma}{\partial \varepsilon}\right)_{ij} = c_{ij} \tag{35}$$

with i and j going from 1 to 2. If j is equal to 3, it means that it is the shear component in the plane of stresses:

$$\left(\frac{\partial \sigma}{\partial \varepsilon}\right)_{ij} = 0. \tag{36}$$

The influence on the shear stress is then investigateded. The linearisation is performed but with respect to the total incremental strain ($\Delta\varepsilon_1$, $\Delta\varepsilon_2$, $\Delta\gamma_{12}$). The basic equation is without plasticity.

$$\partial\sigma_{12} = -G^0_{12}\partial d_{12_{n+1}}\gamma^{\mathrm{e}}_{12_{n+1}} + G^0_{12}(1 - d_{12_{n+1}})\partial\gamma^{\mathrm{e}}_{12_{n+1}} \tag{37}$$

with the variation of damage given by 27, but with

$$\partial Y = \partial Y_{d_{12}} + \alpha_1 \partial Y_{d_1} + \alpha_2 \partial Y_{d_2} \tag{38}$$

with

$$\partial Y_{d_i} = \frac{\sigma_i}{E^0_i}\partial\sigma_i I_i, \tag{39}$$

where I_i depends on the sign of the stress ($I_i = +1$ if $\sigma_i > 0$ else $I_i = 0$ if $\sigma_i < 0$).

$$\partial d = \frac{1}{2}\frac{1}{\sqrt{Y_{n+1}}(\sqrt{Y_{\mathrm{c}}} - \sqrt{Y_0})}(A_{31}\partial\varepsilon_{11} + A_{32}\partial\varepsilon_{22} + A_{33}\partial\varepsilon_{12}), \tag{40}$$

where the different coefficients can be found in Appendix. Then, the variation of the shear stress is found in respect to the different strains:

$$\begin{aligned}\partial\sigma_{12} \;=\; & -G^0_{12}\gamma^{\mathrm{e}}_{12_{n+1}}\frac{1}{2}\frac{1}{\sqrt{Y_{n+1}}(\sqrt{Y_{\mathrm{c}}} - \sqrt{Y_0})}(A_{31}\partial\varepsilon_{11} + \\ & + A_{32}\partial\varepsilon_{22} + A_{33}\partial\gamma_{12}) + G^0_{12}(1 - d_{12_{n+1}})\partial\gamma^{\mathrm{e}}_{12}.\end{aligned} \tag{41}$$

It has to be emphasised that it is valid for carbon fibre. In the case of glass fibre, progressive damage in the direction of the fibre can occur. It is still possible, although more difficult, to express the consistent tangent operator.

4.3.2. *Elastic Plastic Damage Behaviour*

The scheme is modified when plasticity is considered. Firstly, the influence of the incremental is introduced via (21) and (30), so when:

$$\partial\gamma_{12}^{\mathrm{e}} = \partial\gamma_{12} - \partial\gamma_{12}^{\mathrm{p}} \tag{42}$$

then the variation of the damage is reconsidered:

$$\partial d_{12} = \frac{1}{2}\frac{1}{\sqrt{Y_{n+1}}(\sqrt{Y_{\mathrm{c}}} - \sqrt{Y_0})}(A_{31}\partial\varepsilon_{11} + A_{32}\partial\varepsilon_{22} + A_{33}(\partial\gamma_{12} - \partial\gamma_{12}^{\mathrm{p}})). \tag{43}$$

With the consistency condition $\partial f = 0$, we obtain:

$$J_{\mathrm{dp}}G_{12}^{0}(\partial\gamma_{12} - \partial\gamma_{12}^{\mathrm{p}}) - K\gamma p^{\gamma-1}\partial p = 0 \tag{44}$$

and in this particular case:

$$\partial p = J_{\mathrm{ep}}\partial\gamma_{12}^{\mathrm{p}}(1 - d_{12_{n+\beta}}) - \beta|\Delta\gamma_{12}^{\mathrm{p}}|\partial d \tag{45}$$

with these two equations, the variation of damage can be expressed by the function of strain variation, so that:

$$\begin{aligned}
\partial\gamma_{12}^{\mathrm{p}}\Bigg(& J_{\mathrm{dp}}G_{12}^{0} - J_{\mathrm{ep}}(1 - d_{12_{n+\beta}})K\gamma p^{\gamma-1} + \beta|\Delta\gamma_{12}^{\mathrm{p}}| \times \\
& \times \frac{1}{2}\frac{1}{\sqrt{Y_{n+1}}(\sqrt{Y_{\mathrm{c}}} - \sqrt{Y_0})}A_{33}\Bigg) \\
= {} & J_{\mathrm{dp}}G_{12}^{0}\partial\gamma_{12} + K\gamma p^{\gamma-1}\beta|\Delta\gamma_{12}^{\mathrm{p}}| \times \\
& \times \frac{1}{2}\frac{1}{\sqrt{Y_{n+1}}(\sqrt{Y_{\mathrm{c}}} - \sqrt{Y_0})}(A_{31}\partial\varepsilon_{11} + A_{32}\partial\varepsilon_{22} + A_{33}\partial\gamma_{12})
\end{aligned} \tag{46}$$

with

$$\partial\gamma_{12}^{\mathrm{p}} = B_1\partial\varepsilon_{11} + B_2\partial\varepsilon_{22} + B_3\gamma_{12}. \tag{47}$$

The variation of the shear stress with respect to the strain can be expressed by the following equation:

$$\partial\sigma_{12} = C_{31}\partial\varepsilon_{11} + C_{32}\partial\varepsilon_{22} + C_{33}\partial\gamma_{12} \tag{48}$$

so that the consistent tangent matrix is computed. In this context, namely a one-dimensional plastic variable, it can be emphasised that this type of implementation can be used for carbon fibre UD ply with transverse anelastic strain. The variable $\Delta\varepsilon_{\mathrm{T}}^{\mathrm{p}}$ must be introduced in addition to a new equation corresponding to:

$$\Delta\varepsilon_{\mathrm{T}}^{\mathrm{p}}\frac{\partial f}{\partial\sigma_{12}} - \Delta\gamma_{12}^{\mathrm{p}}\frac{\partial f}{\partial\sigma_{\mathrm{T}}} = 0.$$

This equation results from the elimination of the plastic multiplier.

4.4. IMPLEMENTATION IN ABAQUS

The following model was implemented in Abaqus Standard via a user subroutine `umat`. For orthotropic behaviour, Abaqus rotates at the time step of concern, all the variables, namely stresses and strains, in the direction of orthotropy. It means that the computation has to be performed in the direction of the ply. Evolution of the orthotropy frame is not considered and perturbation analysis is performed.

One important point concerning the performance of the resolution is the time step. Abaqus auto adapts the time step. If the convergence is less than three iterations in the time step, then the next time step will be increased automatically. If convergence is poor, between three and ten iterations (values by default), then the time step is kept constant. If convergence is really poor, more than ten iterations, then Abaqus reduces the time step in question. It is possible for the user to modify the time step if:

- poor convergence is encountered in the local algorithm;
- brittle fracture occurs in order to catch the onset of rupture.

5. A Structure: Plate with Hole

The model is tested on a structure. Several assumptions have to be made relating to on numerical and experimental standpoints. The final purpose is to see if the developed model can predict the rupture of the sructure.

5.1. THE EXPERIMENTAL TEST

A 1 mm thick plate (135 $\times$ 50 mm) with a hole of 7 mm radius is stretched between two dies. Several orientations are tested: $[+40, -40]_s$, $[+30, -30]_s$, $[+22.5, -22.5]_s$ (quasi isotropic). A tensile monotonic test is performed. Several measurements are made: the force and the relative displacement are measured every second.

This tensile test is performed on the plate with hole under INSTRON. The main difficulties come from the estimation of boundary conditions. One of the dies is clamped in the machine while the other one is hinged to avoid problems due to misalignment.

5.2. NUMERICAL MODEL

In this part, the geometry is presented as well as the material parameters needed for our model. The whole plate is modelled by a linear quadrilateral element. The material data are given in Table III. To identify the model, tensile tests were performed with different orientations. Some loadings/unloadings were performed in order to identify damage. Once damage was identified, then plasticity could be identified. The method is quite straightforward.

Table III. Identified values for the woven fabric G939/M18.

Material parameter	Values
$E_{11} = E_{22}$	55000 MPa
ν_{12}	0.03
G^0_{12}	3800 MPa
$\sqrt{Y_c}$	4.01 $\sqrt{\text{MPa}}$
$\sqrt{Y_0}$	0.075 $\sqrt{\text{MPa}}$
$\alpha_1 = \alpha_2$	0.16
γ	0.39
R_0	30 MPa
K	600 MPa
Y_{i_f}	6.45 MPa

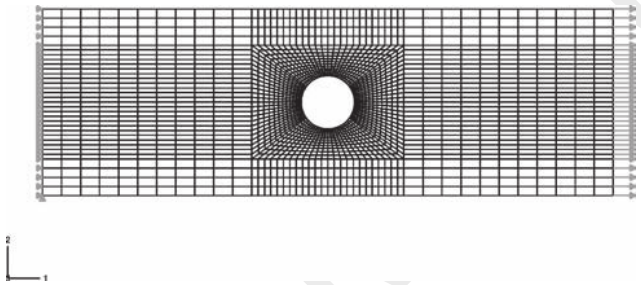

Figure 5. Spatial discretisation of the plate with hole.

The numerical discretised model for the geometry is shown in Figure 5. The boundary conditions are clamped on one side and simply strained on the other. Rigid body motions are avoided by clamping certain degrees of freedom.

To model the laminate, different elements are connected to the same nodes. As a consequence, each element with different material properties is submitted to the same displacement and strains.

5.3. COMPARISON

In this part, the comparison between the numerical results and the experimental measurements will be shown.

The displacement and the force are measured and these variables are extracted from the finite element model. In Figure 6, the comparison is shown.

In this figure, the prediction of the rupture is around 10% from the experimental tests. The validity of the behaviour identified by the material test extrapolated to our structure is quite good. From the numerical stand point, the low number of increments needed to attain the solution are observed, this means that good convergence is assured.

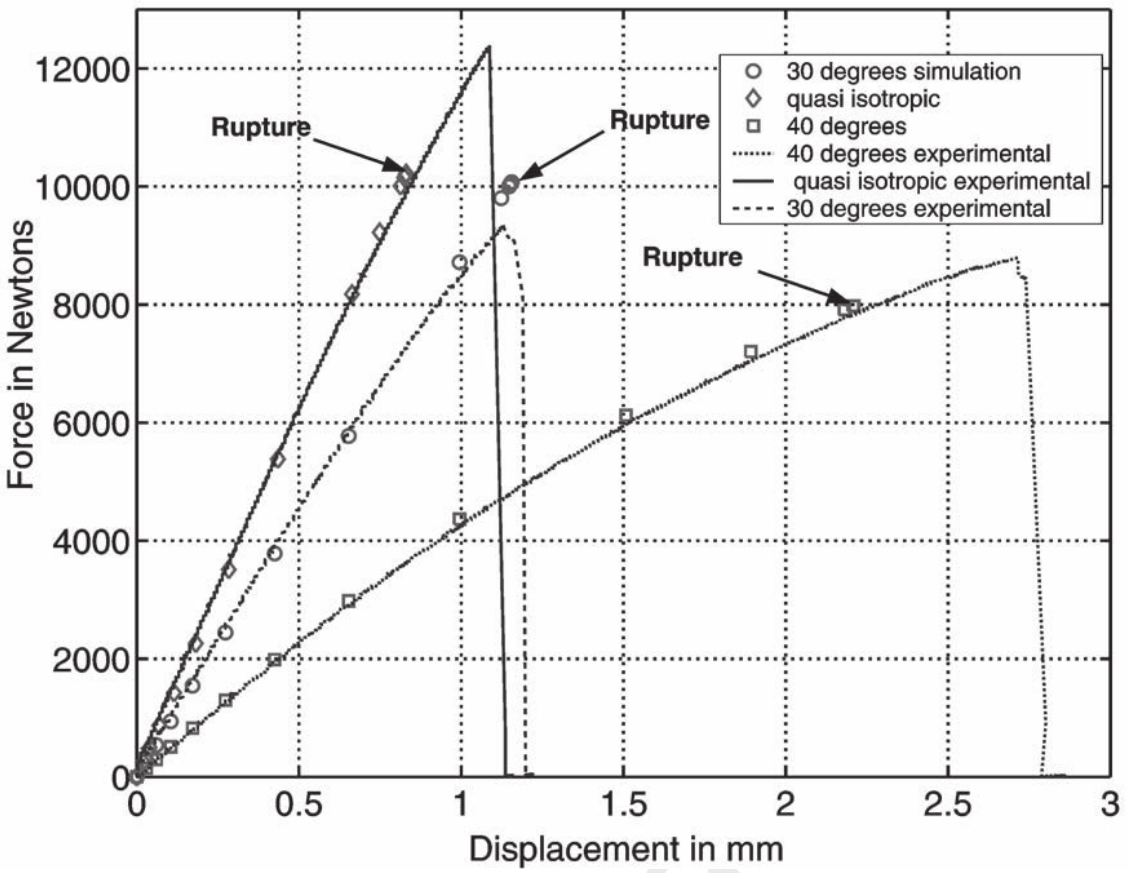

Figure 6. Comparison of the simulation and experiment for different orientations.

For the quasi isotropic structure, the stopping of the calculation is due to brittle rupture in the fibre direction. It was observed that the experiment overpredicted the simulation result. Currently, we are looking at introducing an internal length in order to predict better the fibre direction rupture in the case of structure with high gradient stresses.

For the simulations shown, the interruption of the calculation is due to the fact that the brittle fracture criterion is encountered in the direction of the fibres.

5.4. PERFORMANCE OF THE SCHEME

In order to appreciate the performances of the scheme, two tests were carried out on the structure. The first one corresponded to a small time step and will be seen as the reference solution. The second one was for authorised large time steps. By comparing the two solutions, the performance of the scheme can be appreciated on a $[+45, -45]_s$ structure strained up to 3 mm. In Figure 7, both results are shown. The results are seen to be close to experiments.

Because the consistent tangent operator was computed, the second order of convergence was assured. The total number of iterations by time step were quite small – 2 iterations for the largest increment.

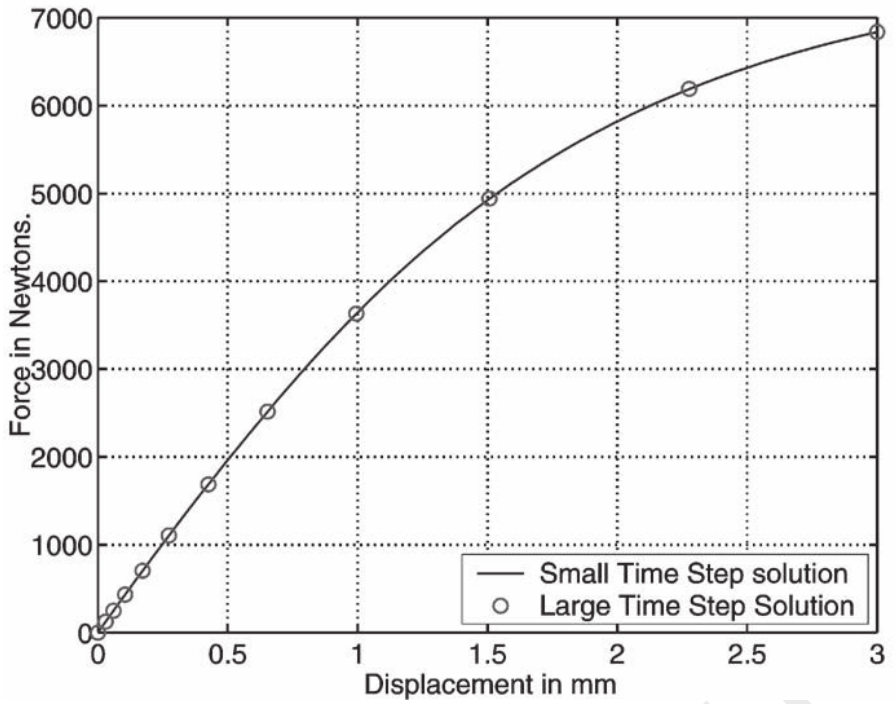

Figure 7. Comparison of the result for small and large time step.

6. Conclusion

In this paper, the numerical implementation of elastic damage plastic behavior of woven ply laminates was carried out. The damage was seen as a lost of rigidity. A fast and simple algorithm was presented and for the orientations shown, the different comparisons seemed to confirm the different assumptions of the model. The scheme showed good performance and in the particular case of woven ply composite with carbon fibre, prediction of the rupture seemed to be coherent. The ongoing developed model plus this numerical procedure, a Euler Backward scheme, enables to optimize structures in an engineering and design department.

Currently, a model for woven ply laminate under fatigue loading [8] is under developement. The next step will concern the implementation of this model in parallel with this routine and will be continally compared to the plate with a hole under cycle loading.

Anyone is interested in this routine can contact the authors.

Appendix: Consistent Tangent Matrix

$$A_{31} = \frac{\alpha_1}{E_1^0}\sigma_1 c_{11} I_1 + \frac{\alpha_2}{E_2^0}\sigma_2 c_{12} I_2, \tag{49}$$

$$A_{32} = \frac{\alpha_1}{E_1^0}\sigma_1 c_{12} I_1 + \frac{\alpha_2}{E_2^0}\sigma_2 c_{22} I_2, \tag{50}$$

$$A_{33} = G_{12}^0 \gamma_{n+1}^{\mathrm{e}}, \tag{51}$$

$$D = J_{\mathrm{dp}} G_{12}^0 - J_{\mathrm{ep}}(1 - d_{12_{n+\beta}}) K \gamma p^{\gamma - 1} +$$

$$+\ \beta|\Delta\gamma_{12}^{\mathrm{p}}|\frac{1}{2}\frac{1}{\sqrt{Y_{n+1}}(\sqrt{Y_{\mathrm{c}}}-\sqrt{Y_0})}A_{33}, \tag{52}$$

$$B_1=\frac{1}{D}K\gamma p^{\gamma-1}\beta|\Delta\gamma_{12}^{\mathrm{p}}|\frac{1}{2}\frac{1}{\sqrt{Y_{n+1}}(\sqrt{Y_{\mathrm{c}}}-\sqrt{Y_0})}A_{31}, \tag{53}$$

$$B_2=\frac{1}{D}K\gamma p^{\gamma-1}\beta|\Delta\gamma_{12}^{\mathrm{p}}|\frac{1}{2}\frac{1}{\sqrt{Y_{n+1}}(\sqrt{Y_{\mathrm{c}}}-\sqrt{Y_0})}A_{32}, \tag{54}$$

$$B_3=\frac{1}{D}\left(J_{\mathrm{dp}}G_{12}^0+K\gamma p^{\gamma-1}\beta|\Delta\gamma_{12}^{\mathrm{p}}|\frac{1}{2}\frac{1}{\sqrt{Y_{n+1}}(\sqrt{Y_{\mathrm{c}}}-\sqrt{Y_0})}A_{33}\right), \tag{55}$$

$$C_{31}=-G_{12}^0(1-d_{12_{n+1}})B_1-$$
$$-\ G_{12}^0\gamma_{12_{n+1}}^{\mathrm{e}}\frac{1}{2}\frac{1}{\sqrt{Y_{n+1}}(\sqrt{Y_{\mathrm{c}}}-\sqrt{Y_0})}(A_{31}-A_{33}B_1), \tag{56}$$

$$C_{32}=-G_{12}^0(1-d_{12_{n+1}})B_2-$$
$$-\ G_{12}^0\gamma_{12_{n+1}}^{\mathrm{e}}\frac{1}{2}\frac{1}{\sqrt{Y_{n+1}}(\sqrt{Y_{\mathrm{c}}}-\sqrt{Y_0})}(A_{32}-A_{33}B_2), \tag{57}$$

$$C_{33}=G_{12}^0(1-d_{12_{n+1}})(1-B_3)-$$
$$-\ G_{12}^0\gamma_{12_{n+1}}^{\mathrm{e}}\frac{1}{2}\frac{1}{\sqrt{Y_{n+1}}(\sqrt{Y_{\mathrm{c}}}-\sqrt{Y_0})}A_{33}(1-B_3). \tag{58}$$

References

1. Reifsnider, K., 'Durability and Damage Tolerance of Fibrous Composite Systems', in *Handbook of Composites*, 2nd edn, Chapman and Hall, 1998, pp. 794–809.
2. Hochard, Ch., Aubourg, P.-A. and Charles, J.-P., 'Modelling of the Mechanical Behaviour of Woven Fabric CFRP Laminates up to Failure', *Composites Science and Technology* **61**, 2001, 221–230.
3. Hochard, Ch., 'Design and Computation of Laminated Composite structures', *Composites and Structures*, accepted, 2003.
4. Singh, A. and Pandey, P. C., 'An Implicit Integration Algorithm for Plane Stress Damage Coupled Elastoplasticity', *Mechanics Research Communications* **26**, 1999, 693–700.
5. de Souza Neto, E. A., 'A Fast, One Equation Integration Algorithm for the Lemaitre Damage Model', *Communications in Numerical Methods in Engineering* **18**, 2002, 541–554.
6. Simo, J. C. and Taylor, R. L., 'Consistent Tangent Operators for Rate Independent Plasticity', *Computer Methods in Applied Mechanics and Engineering* **48**, 1985, 101–118.
7. Ladevèze, P. and Le Dantec, E., 'Damage Modelling of the Elementary Ply for Laminate Composites', *Composites Science and Technology* **43**, 1992, 257–268.
8. Payan, J. and Hochard, C., 'Damage Modelling of Carbon/Epoxy Laminated Composites under Static and Fatigue Loads', *International Journal of Fatigue* **24**, 2002, 299–306.
9. Phillips, E. A., Herakovich, C. T. and Graham, L. L., 'Damage Development in Composites with Large Stress Gradient', *Composites Science and Technology* **61**, 2001, 2169–2182.